Spectral Analysis for Slow Pathway Characterization in Atrioventricular Nodal Reentry Tachycardia

Giorgia Bongiovanni[1], Matteo Fioravanti[2], Francesco Soliani[2], Maria Francesca Notarangelo[3], Cristiana Corsi[1]

[1] Dipartimento di Ingegneria dell'Energia Elettrica e dell'Informazione "Guglielmo Marconi", Università di Bologna, Italia
[2] Biosense-Webster, Roma, Italia
[3] Azienda Ospedaliero-Universitaria di Parma, Italia

Abstract

Despite advancements in supraventricular arrhythmia mapping, ablating atrioventricular nodal reentrant tachycardia (AVNRT) still relies on qualitative identification of slow pathway (SP) potentials. This study aims to characterize SP signals in the frequency domain to improve mapping objectivity.

By analyzing 355 atrial signals from AVNRT ablation patients, a multiparametric analysis of spectral and temporal parameters was conducted to distinguish target from non-target signals.

Combining the amplitude of the second peak with the power spectrum density slope yielded the best discrimination (AUC 0.63), reducing false positives by 50% compared to the operator experience.

Automating SP mapping is crucial to avoid non-target radiofrequency deliveries. Shifting to the frequency domain analysis shows promise and ensures further validation and integration into mapping systems for better ablation strategy planning.

1. Introduction

AVNRT is a common form of supraventricular tachycardia characterized by a reentrant circuit near the atrioventricular (AV) node [1]. The AV node may present two separate pathways for atrial impulses: a faster one in the Koch triangle's front part (in correspondence with the His bundle) and a slower one in the posterior part [2]. AVNRT occurs when the fast pathway conducts impulses quickly with a long refractory period, while the slow pathway conducts impulses more slowly but with shorter recovery times [3].

During normal sinus rhythm, impulses typically travel through the fast pathway. However, if there's an early beat (extrasystole), it may encounter blockage in the fast pathway, leading it to travel through the slow pathway, causing a notable extension in AV node conduction time, often termed a "jump". If the impulse reaches the distal part of the AV node when the fast pathway has recovered, it can activate the fast pathway in reverse, creating a reentrant circuit, potentially resulting in 'slow-fast' AVNRT [4].

Although radiofrequency (RF) current ablation of the fast pathway is effective in eliminating AVNRT, it carries a significant risk of inducing atrioventricular block [5]. For this reason, nowadays the ablation target is the SP, located behind the AV node near the coronary sinus [6]. However, the ongoing challenge is the accurate identification of the SP's location, which depends on the visual assessment and clinical experience of the electrophysiologist.

This work aims to develop a signal classification algorithm to identify the ablation target based on spectral analysis characterization. By analyzing cardiac signals' frequencies, novel insights can be gained, potentially revealing distinctive and predictive parameters not discernible through traditional time-domain evaluation.

2. Materials & Methods

2.1. Population

The dataset comprises 42 patients enrolled at the Azienda Ospedaliero-Universitaria in Parma, Italy, treated for AVNRT using the CARTO 3 electro-anatomic mapping system (version 7.5). The average age was 55 years old with 29 females and 13 males. Each patient underwent effective ablation, with an average of three RF discharges. Twenty-four patients had no prior pharmacological treatment, while 18 received antiarrhythmic therapy.

A total of 355 endocardial signals were analyzed, focusing on Koch's triangle area. Signals included 123 slow pathway (target) signals and 232 non-target signals. Data were collected using Navistar and Smartouch catheters, ensuring reliability with contact force sensors and RF discharge criteria.

2.2. Spectral analysis

Spectral analysis was performed exclusively on the atrial portion of the signal, derived from the corresponding I lead of the ECG, which was previously filtered applying a Butterworth low-pass filter with a cutoff frequency of 30

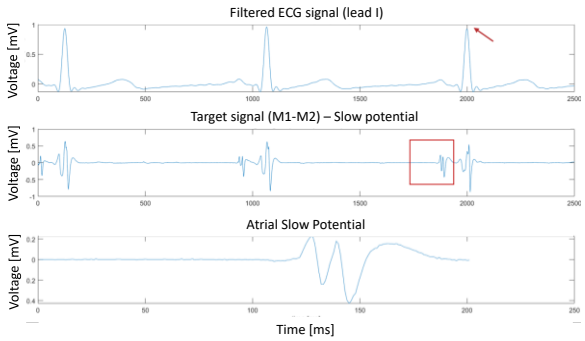

Figure 1. Top panel: a filtered ECG signal (lead I) with the R peak highlighted with a red arrow is shown; middle panel: the full bipolar electrogram used to identify relevant SP in cardiac tissue with the window (red box) is reported; bottom panel: atrial activity within the specific time window describes a focused view for evaluating atrial electrical behavior.

Hz. Subsequently, the last R-wave peak of the trace was identified and a window of [-250, -50] ms relative to the R peak was applied to isolate the final atrial beat within our signal (Figure 1).

The spectral analysis technique decomposes time-domain signals into frequency components, enabling the identification of unique characteristics in target signals compared to non-target ones through the examination of frequencies and intensities. This transformation from time to frequency domain was obtained by applying the Fast Fourier Transform (FFT).

We extracted specific parameters from the amplitude spectrum graph to highlight differences in the SP signal compared to others. These parameters include dominant frequency, amplitude of the dominant peak, frequency of the second peak, amplitude of the second peak, Full Width at Half Maximum (FWHM), the ratio of amplitude between dominant and second peaks, and frequency distance between these peaks (Figure 2). Then we shifted the focus to power spectrum analysis, facilitating the extraction of additional metrics such as two different power spectrum slopes, which describe energy variation across frequencies, and the area under the power spectrum, representing total signal energy across frequencies (Figure 2). The peak-to-peak amplitude in time which measures the voltage difference between the highest and lowest points of a signal within the time domain, indicating the maximum voltage variation was also computed (Figure 3).

2.3. Classification algorithm

The entire signal dataset was split into a training set (70% of the collected signals) to develop our algorithm and a test set (30% of the collected signals) for validation. This ensured both categories were represented proportionally and prevents overfitting.

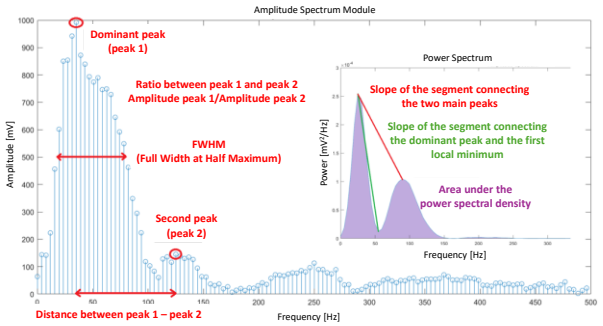

Figure 2. Schematic depiction of the parameters extracted from the signal analysis in the frequency domain. For additional details see the text.

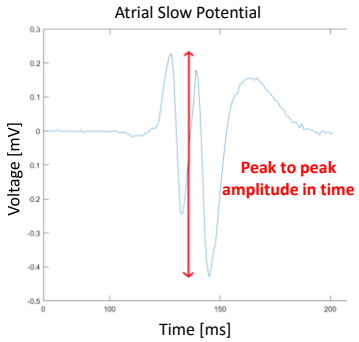

Figure 3. Time-domain waveform of the atrial component of a target signal, with an annotation highlighting the "peak to peak amplitude in time" parameter.

To determine the best parameter combination, we employed a systematic approach, evaluating all possible combinations. This required data normalization using min-max normalization.

Subsequently, we analyzed 2047 parameter combinations iteratively, assigning a weight (w_i) to each parameter (P_i) using the Latin hypercube sampling (LHS) to compute a multiparametric index (MI):

$$MI = \sum_{i=1}^{11} w_i \cdot P_i$$

The multiparametric index was then compared against variable thresholds to estimate the predicted class. Following this step, the Area Under the Curve (AUC) for Receiver Operating Characteristic (ROC) curves for each combination was computed to assess classification performance.

By varying weights up to 1000 times, we identified the optimal combination offering the best classification performance.

The “true” class for each signal was assigned based on the results of the ablation procedure checking on the mapping system which signal was successfully ablated to interrupt AVNRT.

2.4. Validation test

Validation of the classification model's performance beyond the training data is required. In addition, testing our approach on unseen signals could prove the model's ability to generalize predictions to new data, ensuring reliable performance metrics for real-world applications.

In the test phase, we assessed the model's reliability in distinguishing target and non-target signals using the independent dataset. The parameters extracted from the signals were first normalized and the weights computed in the training set were assigned. The multiparametric indices were computed for each signal in the test, and the sensitivity, specificity, and AUC of the ROC curve were calculated.

To evaluate the performance of our classification algorithm compared to the clinical standard based on signal visual assessment, an expert electrophysiologist reviewed all the signals and assigned them to the target/non-target class.

3. Results

Out of the 2047 combinations, the set of parameters that resulted in the best classification performance was obtained using only two parameters: the amplitude of the second peak and the slope of the power spectral density (PSD) from the maximum to the second peak. The weights associated with these parameters obtained applying the LHS were 0.4 and 0.1 respectively and were used to compute the multiparametric index for signal discrimination.

Through meticulous evaluation of the ROC curve computed for the training set (Figure 4), the MI value of 0.1096 corresponding to a sensitivity of 0.80 and a specificity of 0.48 was selected as the threshold to optimize the balance between true positives and true negatives and ensure optimal sensitivity while minimizing false positives.

The testing of the algorithm on an independent dataset showed a slightly lower AUC compared to the training set. The model demonstrated a sensitivity rate of 0.80, correctly identifying 80% of true target signals, crucial for clinical applications. Additionally, it achieved a specificity rate of 0.55, indicating the possibility for improvement in reducing false positives while maintaining a high sensitivity (Figure 5).

Comparison with expert electrophysiologists' performance revealed enhanced accuracy in target signal identification and reduced misclassification rates (sensitivity 0.76 and specificity 0.29). These findings highlight the algorithm's potential to complement clinical decision-making in identifying AVNRT signals with greater precision and confidence.

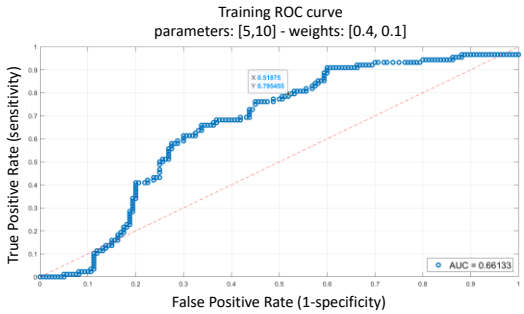

Figure 1. ROC curve obtained in the training set with AUC = 0.66; the threshold corresponding to a sensitivity of 0.80, a specificity of 0.48 and a false positive rate of approximately 0.52 was selected for further testing on the test set.

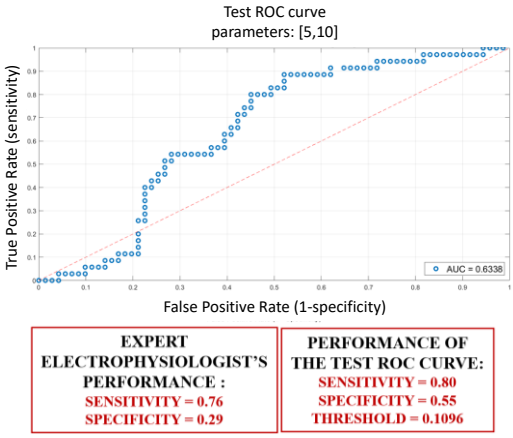

Figure 2. ROC curve obtained in the test set with AUC=0.63, indicating a moderate accuracy of the model in distinguishing between signals during the validation phase. The data reported specifically demonstrate how our algorithm enhances the performance of an expert electrophysiologist, particularly in reducing false positives.

4. Discussion

The study focused on characterizing SP potentials, initially described in the time domain by pioneers like Haissaguerre [6] and Jackman [5]. These signals, known as "Jackman" and "Haissaguerre" potentials, displayed distinct configurations suggesting delayed activation typical of conduction through the SP.

Mapping systems like CARTO utilize voltage mapping techniques to delineate SP areas based on temporal amplitude. Our analysis revealed that temporal amplitude alone is insufficient for precise classification. Therefore, there's a need for a more sophisticated approach to analyzing electrophysiological signals.

In the frequency domain, SP signals exhibited distinctive characteristics, including a dominant peak below 50 Hz and a narrower bandwidth compared to non-target signals. Additionally, target signals often display

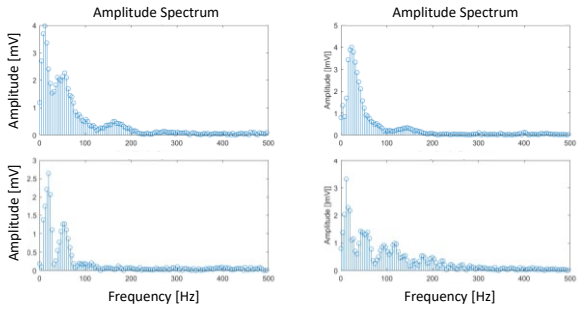

Figure 3. Examples of amplitude spectra of SP signals: each plot displays the energy distribution of the signal across various frequencies, with prominent peaks indicating the dominant frequency components.

secondary peaks with greater amplitudes and lower frequency values. Examples of such characteristic behaviors are shown in Figure 6. These findings underscore the importance of exploring new frontiers in signal analysis to accurately identify SP signals between other complex cardiac signals.

Throughout our analysis, we identified that the amplitude of the second peak, combined with the slope of the PSD from the maximum to the second peak, yielded the best performance. Notably, the amplitude of the second peak played a crucial role in explaining slow pathway signals, resembling Jackman's description of a signal with both slow and sharp components [5]. Our study demonstrated that this sharp component, represented by the second peak in the frequency spectrum, might indicate the presence of a marked high-frequency component, with higher amplitudes in target signals.

Careful parameter selection and weighting were vital in modeling an effective classifier, as evidenced by our ROC curve analysis. Our strategic threshold choice optimized sensitivity and specificity, surpassing expert electrophysiologist performance. Achieving 80% sensitivity and 55% specificity, our model significantly reduced false positives by approximately 50%, enhancing the accuracy of identifying true target signals. This improvement is crucial in preventing unnecessary RF delivery to misclassified signals, enhancing the clinical practice of electrophysiology.

Exploring how relevant frequency domain parameters translate into the time domain could further enrich our understanding of the SP and enhance analysis methodologies, offering electrophysiologists more precise tools for diagnosing and treating SP-related arrhythmias.

5. Conclusions

The results of this work significantly enhance our understanding of SP characterization in AVNRT through spectral analysis. Specifically, parameters like the amplitude of the second peak and the slope of the PSD exhibited notable discriminating power, allowing more precise classification of SP signals.

Our research provides the basis for future innovations, especially the integration of frequency analysis methodologies into clinical protocols that might have the potential to standardize and customize AVNRT treatment.

References

[1] Wu, J., Wu, J., Olgin, J., Miller, J. M., & Zipes, D. P. (2001). Mechanisms Underlying the Reentrant Circuit of Atrioventricular Nodal Reentrant Tachycardia in Isolated Canine Atrioventricular Nodal Preparation Using Optical Mapping. *Circulation Research*, *88*(11), 1189–1195. https://doi.org/10.1161/hh1101.092187

[2] McGuire, M. A., Bourke, J. P., Robotin, M. C., Johnson, D. C., Meldrum-Hanna, W., Nunn, G. R., Uther, J. B., & Ross, D. L. (1993). High-resolution mapping of Koch's triangle using sixty electrodes in humans with atrioventricular junctional (AV nodal) reentrant tachycardia. *Circulation*, *88*(5), 2315–2328. https://doi.org/10.1161/01.CIR.88.5.2315

[3] Wu, D., Denes, P., Dhingra, R., Wyndham, C., & Rosen, K. M. (1975). Determinants of fast- and slow-pathway conduction in patients with dual atrioventricular nodal pathways. *Circulation Research*, *36*(6), 782–790. https://doi.org/10.1161/01.RES.36.6.782

[4] Costantini, M., Carbone, V., & Costantini, L. (2018). Doppia via nodale: basi fisiologiche, risvolti aritmologici ed espressioni elettrocardiografiche. *Giornale Italiano Di Cardiologia*, *19*(4), 222–231.

[5] Jackman, W. M., Beckman, K. J., McClelland, J. H., Wang, X., Friday, K. J., Roman, C. A., Moulton, K. P., Twidale, N., Hazlitt, H. A., Prior, M. I., Oren, J., Overholt, E. D., & Lazzara, R. (1992). Treatment of Supraventricular Tachycardia Due to Atrioventricular Nodal Reentry by Radiofrequency Catheter Ablation of Slow-Pathway Conduction. *New England Journal of Medicine*, *327*(5), 313–318. https://doi.org/10.1056/NEJM199207303270504

[6] Haissaguerre, M., Gaita, F., Fischer, B., Commenges, D., Montserrat, P., d'Ivernois, C., Lemetayer, P., & Warin, J. F. (1992). Elimination of atrioventricular nodal reentrant tachycardia using discrete slow potentials to guide the application of radiofrequency energy. *Circulation*, *85*(6), 2162–2175. https://doi.org/10.1161/01.CIR.85.6.2162

Address for correspondence:

Giorgia Bongiovanni.
Via dell'Università 50, 40057 Cesena (FC), Italy
giorgia.bongiovanni.98@gmail.com